ELSEVIER

Journal of Chromatography A, 769 (1997) 3–24

JOURNAL OF CHROMATOGRAPHY A

Optimal operation of simulated moving bed units for nonlinear chromatographic separations

Marco Mazzotti[a], Giuseppe Storti[b], Massimo Morbidelli[c,*]

[a]*Dipartimento di Chimica, Politecnico di Milano, Via Mancinelli, 7, 20131 Milan, Italy*

[b]*Dipartimento di Ingegneria Chimica e Materiali, Università degli Studi di Cagliari, Piazza d'Armi, 09123 Cagliari, Italy*

[c]*Laboratorium für Technische Chemie LTC, ETH Zentrum, CAB C40, Universitätstrasse 6, CH-8092 Zurich, Switzerland*

Abstract

The simulated moving bed (SMB) technology is receiving more and more attention as a convenient technique for the production scale continuous chromatographic separation of fine chemicals. Characteristic features of SMBs are improved performances with respect to preparative chromatography and nonlinear competitive adsorption behavior. The selection of the operating conditions to achieve high separation performances under nonlinear conditions is acknowledged to be the major problem in running a SMB unit for a new application. This problem is solved in this paper, where a general theory is developed which provides explicit criteria for the choice of the operating conditions of SMB units to achieve the prescribed separation of a mixture characterized by both constant selectivity Langmuir isotherms and variable selectivity modified Langmuir isotherms. The space of the operating parameters, i.e. the fluid to solid flow-rate ratios, is divided in regions with different separation regimes. The effect of increasing nonlinearity of the system on the operating conditions and the separation performances, namely desorbent requirement, enrichment, productivity and robustness of the separation, is thoroughly analyzed. The obtained results are shown to provide a very convenient tool to find both optimal and robust operating conditions of SMB units. Finally, a comparison between model predictions and experimental data dealing with the resolution of different racemic mixtures assesses the reliability and accuracy of the obtained theoretical findings.

Keywords: Simulated moving bed chromatography; Preparative chromatography; Adsorption isotherms; Non-linear chromatography

1. Introduction

Chromatography is a widely adopted separation technique, which is acquiring greater and greater interest in particular for preparative applications. In this context the simulated moving bed (SMB) technology [1] has demonstrated its considerable advantages with respect to classical preparative chromatography methods. In fact, its adoption is no more limited to hydrocarbon and sugar separations as in the period from the 1960s to the 1980s [2], but is being extended to fine chemistry applications such as separations of natural products, pharmaceuticals and aroma. Among these, many examples deal with the resolution of racemates, which is indeed becoming one of the major fields of application of SMBs [3,4].

The SMB unit is a continuous process apparatus, whose principle of operation can be best described with reference to the equivalent true counter-current (TCC) (or true moving bed) configuration illustrated in Fig. 1. This is divided in four sections (this is the most widely adopted configuration even though two and three section units, also, can be applied [1,5]), each one playing a specific role in the separation.

*Corresponding author.

PII S0021-9673(97)00048-4

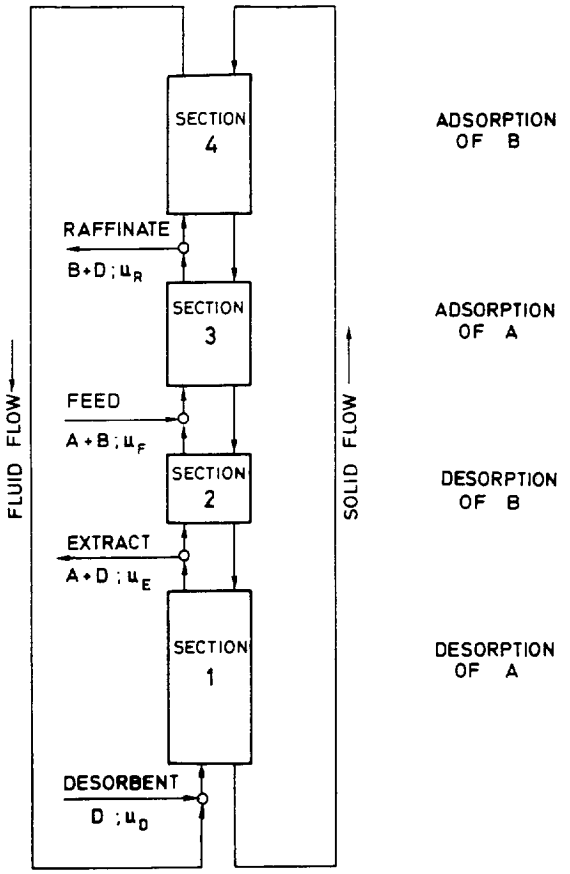

Fig. 1. Scheme of a four section true counter-current unit for continuous adsorptive separations: the binary separation of a strongly adsorbed component A and a weakly adsorbed component B is considered.

Let us consider a feed mixture containing a proper inert solvent and the two components to be separated: the more adsorbable component, called A, which is to be collected in the extract stream, and the less adsorbable one, called B, to be collected in the raffinate stream. The separation is carried out in the two central sections, where component A is conveyed downwards to the extract outlet and component B upwards to the raffinate outlet, respectively. The desorbent, which in the cases of interest in fine chemistry applications is in general the solvent itself, is fed to the bottom of section 1, so as to elute component A and regenerate the adsorbent solid that is then recycled to the top of section 4. Finally, component B is adsorbed in the fourth section of the unit, so as to regenerate the desorbent, which is mixed with the make-up desorbent stream and recycled to column 1, as explained above.

The TCC configuration is not an efficient process scheme because of the difficulties caused by the movement of the solid phase. Therefore, in practical applications the solid beds are fixed and the continuous movement of the adsorbent solid is simulated by a periodic shift of the inlet and outlet ports of the unit in the same direction as the fluid phase flow, thus yielding the SMB configuration illustrated in Fig. 2. Each section of the SMB unit is divided in several subsections (5-1-3-3 for example in Fig. 2) in order to closely approximate the counter-current movement of the solid phase. Each one of these consists of a fixed bed fed by the fluid stream from the preceeding subsection after mixing with or withdrawal of an external stream, as required.

Due to their continuous counter-current nature, after the start up transient TCC units achieve a steady state, where every process variable remains constant in each location in the unit. On the contrary, the stationary regime of a SMB unit is a cyclic steady state, in which the unit exhibits the same time

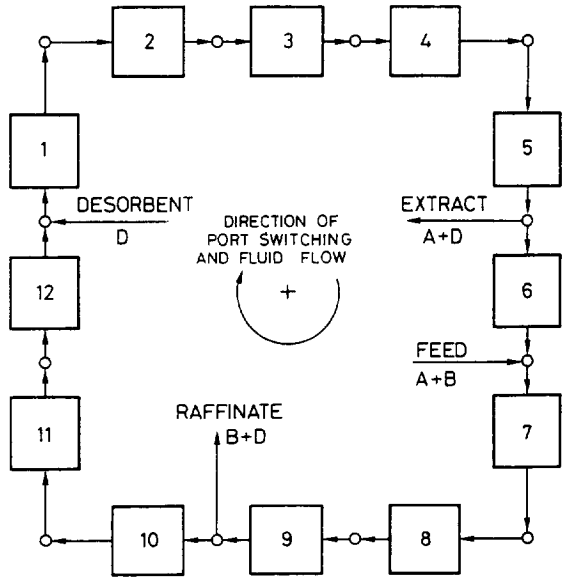

Fig. 2. Scheme of a four-section simulated moving bed unit for continuous adsorptive separations with port distribution 5-1-3-3.

dependent behavior during each time period between two successive switches of the inlet and outlet ports (cf. [6] for this and other features of the dynamic behavior of SMB units). Therefore, in order to model the stationary regime of a SMB unit a time dependent model is required, whereas for a TCC unit a time independent model is enough. Since the two unit configurations are equivalent, i.e. they achieve the same separation performances provided geometric and kinematic conversion rules are fulfilled, the simpler model of the equivalent TCC unit can be used to predict the steady state separation performances of SMB units, in particular for design purposes. The above mentioned conversion rules are given by the following relationships:

$$V_j = S_j V \tag{1}$$

$$\frac{V}{t^*} = \frac{Q_s}{1-\varepsilon} \tag{2}$$

$$Q_j^{SMB} = \left[Q_j^{TCC} + \frac{Q_s \varepsilon}{1-\varepsilon} \right] \tag{3}$$

where V_j and V are the volume of the jth section of the TCC unit and of the fixed bed of the SMB unit, respectively; S_j is the number of subsections in the jth section of the SMB unit; t^* is the switch time of the SMB unit, i.e. the time period between two successive switches of the inlet and outlet ports; ε is the void fraction of the bed; Q_s is the volumetric solid flow-rate in the TCC unit; Q_j^{SMB} and Q_j^{TCC} are the volumetric flow-rates in the SMB unit and in the equivalent TCC unit, respectively. This equivalence will be extensively exploited in the following.

SMB units exhibit a number of advantages with respect to batchwise preparative chromatography. In particular, these are due to the continuous nature of the operation and to an efficient use of the stationary and mobile phases, which allows the decrease of the desorbent requirement and the improvement of the productivity per unit time and unit mass of stationary phase. Solvent savings up to 90% and increases of productivity up to several times have been reported [3,7–9]. Moreover, high performances can be achieved even at rather low values of selectivity (as low as 1.05) and with a relatively small number of theoretical plates [10]. These features of SMB units are essentially due to the fact that, contrary to preparative chromatography, the concentration profiles of the components to be separated are allowed to overlap along the adsorption beds, being required that the components are pure only at the extract and raffinate outlet locations. This allows operation in concentration overload conditions, i.e. in the nonlinear range of the adsorption isotherm, thus optimizing the separation performances. All these positive features are particularly attractive in the case of enantiomer separations, where the application of SMB technology is bound to be most rewarding in terms of reduction of development times and production costs of optically pure products and in terms of increase of availability, recovery and purity of both enantiomers [3].

From the adsorption thermodynamics point of view, concentration overload conditions imply that the system exhibits nonlinear competitive behavior. This must be carefully accounted for when the operating conditions, i.e. flow-rates and switching time, are chosen to achieve the desired separation performances. Simple design criteria exist for the separation of mixtures in the linear regime [1], but it is well known that they are of little use when nonlinear effects must be accounted for [9–11]. This is indeed one of the main problems in operating SMB units for new applications to fine chemicals separations.

In this work, we address this issue and present a general theory for the design of operating conditions of SMB units operating in the nonlinear regime [11–14]. In particular we apply it to the case illustrated in Figs. 1 and 2 which is of interest here, namely the separation of a binary mixture using a desorbent which can be assumed to be inert, or nonadsorbable. In Section 2 the theoretical framework in which our analysis is carried out is described and explicit criteria for the choice of complete separation operating conditions are derived. After defining the main performance parameters and introducing the concept of robust operating conditions in Section 3, in Section 4 the role of nonlinearity in determining separation performances is thoroughly analyzed, with particular reference to the nonlinear effects due to changes of the composition of the feed mixture. Finally, in Section 5 these theoretical results are assessed by comparison with different sets of experimental data reported in the literature.

2. Design of operating conditions to achieve complete separation

In developing a new SMB application two design issues must be addressed. The first one deals with the size of the unit, namely the number of columns and their length and diameter, and the particle size distribution of the adsorbent solid. Depending on the required production rate the above mentioned parameters are chosen with the aim of optimizing column efficiency and productivity while keeping pressure drop below a given upper bound [10]. The second issue arises when a SMB unit is already available and the objective is to use it with the aim of performing a new separation. In the latter case the operating conditions must be chosen so as to achieve the prescribed separation performances.

In this work we address the second issue; in particular we assume that the SMB unit and its geometric and packing parameters are fixed and that the adsorption equilibrium properties of the components to be separated are known. Therefore, the operating parameters to be selected are the internal flow-rates, Q_j, the switch time, t^* [corresponding to the solid flow-rate, Q_s, in the equivalent TCC unit according to Eq. (2)] and the feed composition. In most cases, this implies the choice of the overall feed concentration, c_T^F, only, since the relative composition of the two components to be separated is fixed. This is the case for example when a racemic mixture must be resolved. However, there are situations where also the relative composition of the two components can be changed before feeding the SMB separation unit. This may occur when the SMB unit has an upstream reaction step whose selectivity and conversion can be tuned rather freely or else when the adsorptive separation is coupled with another separation pretreatment whose degree of refinement can also be selected at will. Both possibilities will be accounted for in the following analysis.

The classical approach to the selection of the operating conditions consists of the application of a McCabe–Thiele-like analysis to an ideal stage-by-stage model of the unit [15,16]. This can be applied to systems described by any kind of adsorption isotherm, but is limited to binary separations, unless some kind of short-cut method is adopted. A different approach can be developed [11,12,14], which is based on the equilibrium theory model, where axial mixing and mass transport resistances are neglected and adsorption equilibrium is assumed to be established everywhere at every time in the column.

In this framework, the equivalent TCC configuration is considered and the model equations of the four-section TCC unit in Fig. 1 are constituted of four sets of material balance equations, one for each section j, together with the relevant boundary conditions and the material balances at the column ends and at the nodes of the unit [11,17]. With reference to a binary separation, the material balance equations are given by the following set of first-order partial differential equations:

$$\frac{\partial}{\partial \tau}[\varepsilon^* c_i^j + (1-\varepsilon^*) n_i^j] + (1-\varepsilon_p)\frac{\partial}{\partial \xi}[m_j c_i^j - n_i^j] = 0, \quad (i = \mathrm{A}, \mathrm{B}) \tag{4}$$

where $\tau = tQ_s/V$ and $\xi = Y/V$ are the dimensionless time and space coordinates; $\varepsilon^* = \varepsilon + \varepsilon_p(1-\varepsilon)$ is the overall void fraction of the bed, whereas ε_p is the intraparticle porosity. In these equations, the composition of the adsorbed phase, n_i^j, is calculated according to the equilibrium relationship as a function of the fluid phase composition:

$$n_i^j = f_i^{eq}(c_A^j, c_B^j), \quad (i = \mathrm{A}, \mathrm{B}) \tag{5}$$

The parameters m_j are the so-called flow-rate ratios and are defined as the ratio of the net fluid flow-rate over the solid phase flow-rate in each section of the unit:

$$m_j = \frac{\text{net fluid flow} - \text{rate}}{\text{adsorbed phase flow} - \text{rate}} = \frac{Q_j^{TCC} - Q_s\varepsilon_p}{Q_s(1-\varepsilon_p)} \tag{6}$$

Alternatively, these can be defined in terms of the operating parameters of the equivalent SMB unit using the conversion rules (2) and (3):

$$m_j = \frac{Q_j^{SMB} t^* - V\varepsilon^*}{V(1-\varepsilon^*)} \tag{7}$$

In the case of linear and Langmuir adsorption equilibrium isotherms, equilibrium theory demonstrates that the model of a single counter-current adsorption column, i.e. the set of Eqs. (4) and (5) for

a specific value of j with given constant initial and boundary conditions, predicts that the column achieves a homogeneous steady state whose composition is selected by the value of the flow-rate ratio, m_j [18]. Accordingly, the steady state regime of a four-section TCC unit, as well as the corresponding cyclic steady-state regime of the equivalent SMB unit, depends only on the feed composition and on the values of the four flow-rate ratios m_j, $j=1,...,4$. It follows that, given the feed composition, in the framework of equilibrium theory the design problem for either TCC or SMB units reduces to developing criteria for the selection of the values of the m_j parameters [11].

Let us consider the process requirement of complete separation; by this the situation illustrated in Figs. 1 and 2 is referred to, where the strong and weak components are collected each in the prescribed outlet stream only, i.e. extract and raffinate, respectively. Only specific combinations of constant states are compatible with complete separation and the conditions to be enforced on the flow-rate ratios in order to achieve these can be derived from equilibrium theory (for the sake of brevity we omit the details of this derivation; the interested reader can find them elsewhere [11,12]). According to the description of the behavior of the TCC unit given above these constraints imply that in the two central sections the net flow-rates of components A and B must be negative and positive, respectively, and that in sections 1 and 4 the net flow-rates of both components must be positive and negative, respectively. Complete separation can also be regarded as the operating regime where both outlet streams exhibit 100% purity, being purities defined as follows:

$$P_E = \frac{100 c_A^E}{c_A^E + c_B^E} \tag{8}$$

$$P_R = \frac{100 c_B^R}{c_A^R + c_B^R} \tag{9}$$

2.1. Linear systems

First, let us consider the case of systems described by the linear adsorption isotherm:

$$n_i = H_i c_i, \quad (i = A, B) \tag{10}$$

where H_i is the Henry constant of the ith component. Following the procedure summarized above, it is easy to prove the well known result that in this simple case the necessary and sufficient conditions for complete separation are the following inequalities:

$$H_A < m_1 < \infty \tag{11}$$

$$H_B < m_2 < H_A \tag{12}$$

$$H_B < m_3 < H_A \tag{13}$$

$$\frac{-\varepsilon_p}{(1-\varepsilon_p)} < m_4 < H_B \tag{14}$$

These constraints define a region in the four-dimensional space whose coordinates are the operating parameters m_1, m_2, m_3 and m_4 and whose points represent operating conditions corresponding to complete separation. It is noteworthy that these do not depend on feed composition; since the linear isotherm mostly applies when the relevant species are very diluted, constraints (11) to (14) implicitly refer to infinite dilution conditions.

It is worth considering sections 2 and 3 of the TCC unit, which play a key role in performing the separation. A positive feed flow-rate implies $m_3 > m_2$ and the constraints (12) and (13) can be rewritten as follows:

$$H_B < m_2 < m_3 < H_A \tag{15}$$

These inequalities define the projection of the four-dimensional region of complete separation onto the (m_2, m_3) plane shown in Fig. 3. Furthermore, it is useful to analyze the whole plane in terms of purities of the product streams. First, note that the region where the separation can be pursued is constrained by $m_2 < H_A$ and $m_3 > H_B$; if either the former or the latter inequality is not fulfilled either the extract or the raffinate outlet, respectively, is flooded with solvent and no separation is obtained. Moreover, the region of the (m_2, m_3) plane where the separation can take place is divided in three more regions beside the triangle-shaped complete separation region. The region where $m_3 > H_A$ and $H_B < m_2 < H_A$ is constituted of operating points corresponding to conditions for which the constraint (13) is not

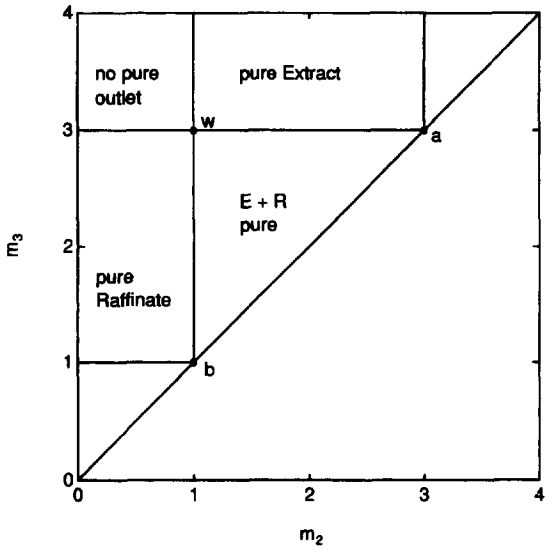

Fig. 3. Regions of the (m_2, m_3) plane with different separation regimes in terms of purity of the outlet streams, for a system described by the linear adsorption isotherm (10): $H_A = 3$; $H_B = 1$.

fulfilled, hence the strong component A is carried upwards, thus polluting the raffinate stream, whose purity drops below 100%, whereas P_E is still 100%. For similar reasons the region where $m_2 < H_B$ and $H_B < m_3 < H_A$ corresponds to operation where $P_R = 100\%$ whereas $P_E < 100\%$. The region where both $m_3 > H_A$ and $m_2 < H_B$ corresponds to operating conditions for which both components distribute in the two product streams and both purity values drop below 100%.

These results can be summarized by stating that in the frame of equilibrium theory, if the flow-rate ratios m_1 and m_4 fulfil their relevant constraints (11) and (14), the consideration of the relative position of the operating point in the (m_2, m_3) plane with respect to the four regions of separation allows to make a prediction of the separation performance of the unit.

2.2. Nonlinear systems: constant selectivity Langmuir isotherm

Now, let us consider a separation which involves two species whose adsorption equilibrium properties can be described by means of the competitive nonstoichiometric Langmuir isotherm:

$$n_i = q_i = \frac{N_i K_i c_i}{1 + K_A c_A + K_B c_B}, \quad (i = A, B) \tag{16}$$

where K_i and N_i are the equilibrium constant and the saturation loading capacity of the i-th species, respectively. Notice that the symbol q_i is used to represent the functional relationship on the right hand side of the previous equation; it will be used in the following with this meaning. Moreover, let us define the adsorptivity $\gamma_i = N_i K_i$.

It is worth rewriting the model Eqs. (4,5) in the case of a system described by the Langmuir isotherm (16):

$$\frac{\partial}{\partial \tau}[\varepsilon^* c_i^j + (1 - \varepsilon^*) q_i^j] + (1 - \varepsilon_p)\frac{\partial}{\partial \xi}[m_j c_i^j - q_i^j] = 0 \quad (i = A, B) \tag{17}$$

In this equation the equilibrium adsorbed phase concentration is given by Eq. (16) rather than by the generic Eq. (5) and this has been emphasized in Eq. (17) by using the symbol q_i instead of n_i as in the original Eq. (4). In the frame of equilibrium theory Eq. (17) can be solved analitically for constant initial and boundary conditions [18].

Applying the method briefly summarized at the end of Section 2 allows the derivation of the following necessary and sufficient conditions on the flow-rate ratios m_j to achieve complete separation [11,12,14]:

$$\gamma_A = m_{1,\min} < m_1 < \infty \tag{18}$$

$$m_{2,\min}(m_2, m_3) < m_2 < m_3 < m_{3,\max}(m_2, m_3) \tag{19}$$

$$\frac{-\varepsilon_p}{1 - \varepsilon_p} < m_4 < m_{4,\max}(m_2, m_3) = \frac{1}{2}\left\{\gamma_B + m_3 + K_B c_B^F (m_3 - m_2) - \sqrt{[\gamma_B + m_3 + K_B c_B^F (m_3 - m_2)]^2 - 4\gamma_B m_3}\right\} \tag{20}$$

The lower bound on m_1 and the upper bound on m_4 are explicit. However, the former does not depend on the other flow-rate ratios, whereas the latter is an explicit function of the flow-rate ratios m_2 and m_3.

Though implicit, the constraints (19) on m_2 and m_3 do not depend on m_1 and m_4. Hence they define

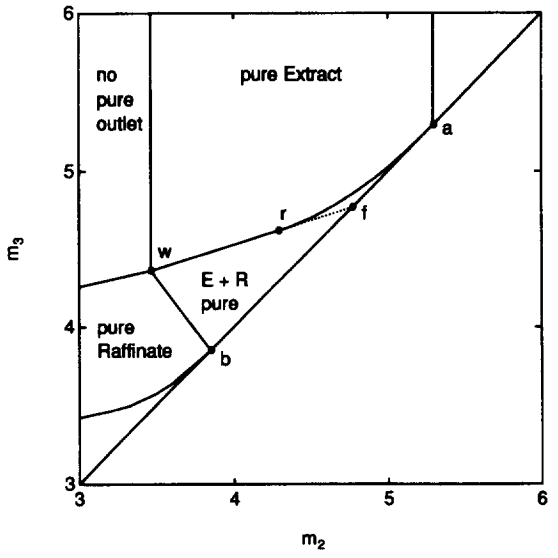

Fig. 4. Separation of a two component mixture using a nonadsorbable desorbent. Regions of the (m_2, m_3) plane with different separation regimes in terms of purity of the outlet streams, for a system described by the nonstoichiometric Langmuir adsorption isotherm (16): $N_A = 165$ g/l, $N_B = 220$ g/l, $K_A = 0.0321$ l/g, $K_B = 0.0175$ l/g, $c_A^F = 5$ g/l, $c_B^F = 5$ g/l.

the complete separation region in the (m_2, m_3) plane, which is the triangle-shaped region illustrated in Fig. 4, whose explicit boundaries are reported below:

- Straight line wf:

$$[\gamma_A - \omega_G(1 + K_A c_A^F)]m_2 + K_A c_A^F \omega_G m_3 = \omega_G(\gamma_A - \omega_G) \quad (21)$$

- Straight line wb:

$$[\gamma_A - \gamma_B(1 + K_A c_A^F)]m_2 + K_A c_A^F \gamma_B m_3 = \gamma_B(\gamma_A - \gamma_B) \quad (22)$$

- Curve ra:

$$m_3 = m_2 + \frac{(\sqrt{\gamma_A} - \sqrt{m_2})^2}{K_A c_A^F} \quad (23)$$

- Straight line ab:

$$m_3 = m_2 \quad (24)$$

The coordinates of the intersection points are given by:

$$\text{point a} \quad (\gamma_A, \gamma_A) \quad (25)$$

$$\text{point b} \quad (\gamma_B, \gamma_B) \quad (26)$$

$$\text{point f} \quad (\omega_G, \omega_G) \quad (27)$$

$$\text{point r} \quad \left(\frac{\omega_G^2}{\gamma_A}, \frac{\omega_G[\omega_F(\gamma_A - \omega_G)(\gamma_A - \gamma_B) + \gamma_B \omega_G(\gamma_A - \omega_F)]}{\gamma_A \gamma_B(\gamma_A - \omega_F)} \right) \quad (28)$$

$$\text{point w} \quad \left(\frac{\gamma_B \omega_G}{\gamma_A}, \frac{\omega_G[\omega_F(\gamma_A - \gamma_B) + \gamma_B(\gamma_B - \omega_F)]}{\gamma_B(\gamma_A - \omega_F)} \right) \quad (29)$$

It is worth noting that the above equations depend on the feed composition through the parameters ω_F and ω_G, which are given by the roots of the following quadratic equation $(\omega_G > \omega_F > 0)$:

$$(1 + K_A c_A^F + K_B c_B^F)\omega^2 - [\gamma_A(1 + K_B c_B^F) + \gamma_B(1 + K_A c_A^F)]\omega + \gamma_A \gamma_B = 0 \quad (30)$$

It is of key importance to underline that even though the above equations are derived through a rather difficult mathematical procedure the final result is simply a set of algebraic expressions that can be very easily applied. Moreover, the topological structure of the regions of separation in the (m_2, m_3) plane illustrated in Fig. 4 is similar to that obtained in the linear case. In fact, also in the nonlinear case there are three different separation regions around the complete separation one, as illustrated in Fig. 4; proceeding clockwise from the lower left corner of the (m_2, m_3) plane there can be found the pure raffinate region, the no pure outlet region and the pure extract region. However, the differences are important; in particular the boundaries of the complete separation region in the Langmuir case depend on the feed composition and the constraints on the flow-rate ratios are coupled and not independent as in the linear case. It is noteworthy that the information provided by the geometrical representation of the separation regions in the (m_2, m_3) plane can be directly applied only if the constraints on m_1 and m_4, i.e. inequalities (18) and (20), are fulfilled.

Two important features of the Langmuir isotherm (16) are worth underlying. The first one is that it characterizes constant selectivity systems; in fact the selectivity of the strong component A with respect to the weak component B is given by:

$$S_{AB} = \frac{n_A/n_B}{c_A/c_B} = \frac{\gamma_A}{\gamma_B} \tag{31}$$

which is a composition independent ratio.

The second feature is that in the limit of very low fluid phase concentrations, i.e. when both c_A and c_B tend to zero, the Langmuir isotherm (16) approaches the linear isotherm (10) with $H_i = \gamma_i$. Therefore this adsorption equilibrium relationship is well suited to study the transition from linear to nonlinear behavior. This transition can be obtained by simply changing the concentration values; in the case of SMB separations this corresponds to changing the overall feed concentration $c_T^F = c_A^F + c_B^F$.

2.3. Nonlinear systems: variable selectivity modified Langmuir isotherm

Sometimes, the assumption of constant selectivity is unacceptable and more complex adsorption isotherms than the Langmuir isotherm must be used [19]. A variable selectivity adsorption isotherm which is often adopted in the field of adsorptive separation of enantiomers is obtained by adding a linear term to the Langmuir isotherm; this is the so-called modified Langmuir isotherm [3]. Although in principle the coefficient of the linear term is different for different species, in many practical cases it is assumed to be the same for both enantiomers, thus obtaining the following expression [10]:

$$n_i = hc_i + \frac{N_i K_i c_i}{1 + K_A c_A + K_B c_B} = hc_i + q_i, \quad (i = A, B) \tag{32}$$

where q_i is given by Eq. (16). In this case the selectivity is composition dependent, being given by the following ratio:

$$S_{AB} = \frac{h(1 + K_A c_A + K_B c_B) + \gamma_A}{h(1 + K_A c_A + K_B c_B) + \gamma_B} \tag{33}$$

Note however that if $\gamma_A > \gamma_B$, then $S_{AB} > 1$ for any composition of the system, i.e. this model is not capable to describe a system exhibiting an azeotrope [19]. Also the modified Langmuir isotherm approaches the linear model when the concentration of the two species tend to zero; in this case $H_i = h + \gamma_i$.

The importance of this model stems from the fact that although selectivity is composition dependent, nevertheless it is possible to develop explicit criteria to select the operating conditions of SMB units to achieve complete separation. In practice these criteria can be simply derived from those obtained in the previous section for the Langmuir isotherm (16). In order to demonstrate this, let us substitute the modified Langmuir isotherm (32) into the equilibrium theory model Eq. (4) and Eq. (5), thus obtaining:

$$\frac{\partial}{\partial \tau}\left\{[\varepsilon^* + (1-\varepsilon^*)h]c_i^j + (1-\varepsilon^*)q_i^j\right\} + (1-\varepsilon_p)\frac{\partial}{\partial \xi}\left\{(m_j - h)c_i^j - q_i^j\right\} = 0, \quad (i = A, B) \tag{34}$$

This equation has the same mathematical structure as Eq. (17). In particular, the expressions giving the total concentrations appearing within the time derivatives in Eqs. (17) and (34) are different, thus indicating that the dynamical behaviors predicted by the two models are different, as expected. Since we are interested in the steady state solutions, which depends only on the space derivative term in Eq. (17) and on the initial and boundary conditions, the space derivative is the only one which matters in this context. It can readily be noticed that the space derivatives in Eqs. (17) and (34) have the same expressions, provided that the flow-rate ratio m_j in Eq. (17) is substituted by the modified flow-rate ratio m_j' in Eq. (34):

$$m_j' = m_j - h \tag{35}$$

It follows that the same single section steady state solution of the equilibrium theory model for the Langmuir isotherm (16) applies to the model using the modified Langmuir isotherm (32) provided that m_j' is used instead m_j. Accordingly, the complete separation region for the counter-current adsorptive separation of a system described by the modified Langmuir isotherm in the space whose coordinates are the modified flow-rate ratios m_j', is given by the same Eqs. (18–29) derived for the Langmuir isotherm using the K_i and N_i parameters of the modified Langmuir isotherm. The complete separation region in the space spanned by the flow-rate ratios m_j is

obtained by shifting the one obtained in the m_j' space of a quantity equal to the value of the linear term coefficient h.

2.4. Nonlinear multicomponent systems

The results reported in the previous sections for binary separations using the Langmuir and the modified Langmuir isotherms can be further generalized. As a matter of fact, for the same isotherms they can be extended to multicomponent separations where the desorbent is not necessarily inert, but it may exhibit any adsorptivity with respect to the components to be separated [5,14].

Explicit criteria for the design of operating conditions of continuous counter-current adsorptive separation units can be obtained also for systems characterized by the stoichiometric constant selectivity Langmuir isotherm:

$$n_i = \frac{NK_i c_i}{\sum_{j=1}^{NC} K_j c_j}, \quad (i = 1,...,NC) \tag{36}$$

where N is the saturation loading capacity, which is assumed to be the same for all components of the fluid mixture, and NC is the number of adsorbable components. Also in this case multicomponent separations and desorbents having any adsorptivity (but not null) with respect to the feed components can be accounted for [11,12,20].

3. Optimal and robust operating conditions

In the previous section the performances of continuous counter-current adsorptive separation units have been evaluated accounting for purity of the product streams only. In practice other performance parameters must be considered in order to determine the optimal operating conditions within the complete separation regions. In the following, important parameters, such as desorbent requirement, enrichment and productivity, are defined and discussed. However, operating conditions may optimize the performance parameters and at the same time turn out to be not feasible on the basis of different considerations. These are concerned with the ability of the system to keep the same qualitative operating regime in the presence of different kinds of disturbances. This is the issue of robust operating conditions, that will be discussed in Section 3.3.

3.1. Performance parameters

3.1.1. Desorbent requirement

With reference to the process scheme in Fig. 1, it can be observed that during the separation there is a net consumption of desorbent. This is fed to the unit both in the feed stream, as the solvent of the components to be separated, and in the make-up desorbent stream, in order to compensate the desorbent lost in the product streams. Desorbent requirement, DR, is defined as the mass of desorbent used to recover a unit mass of pure product:

$$\mathrm{DR} = \frac{(Q_D + Q_F)c^D}{Q_F c_T^F} \tag{37}$$

where Q_D and Q_F are the make-up desorbent and the feed flow-rates, respectively; c^D and c_T^F are the desorbent density and the overall concentration of the components to be separated in the feed, respectively. Also note that it has been assumed that the feed mixture is rather diluted, as it is the case in most applications, so that the feed density is not very different from the desorbent density. Expressing the flow-rates in terms of flow-rate ratios yields the following relationship:

$$\mathrm{DR} = \frac{c^D}{c_T^F}\left(1 + \frac{m_1 - m_4}{m_3 - m_2}\right) \tag{38}$$

3.1.2. Enrichment

Besides purity, which according to its definitions (8) and (9) refers to the desorbent free concentration of the desired component in the relevant outlet stream, its absolute concentration is also important and should be maximized. The corresponding performance parameter is called enrichment and is defined as the ratio of the outlet concentration over the feed concentration of the desired component. In the case of a binary separation, the enrichments of A and B are defined accordingly and under the assumption of complete separation can be usefully expressed in terms of flow-rate ratios as follows:

$$E_A = \frac{c_A^E}{c_A^F} = \frac{m_3 - m_2}{m_1 - m_2} \tag{39}$$

$$E_B = \frac{c_B^E}{c_B^F} = \frac{m_3 - m_2}{m_3 - m_4} \tag{40}$$

3.1.3. Productivity

In general, an optimal procedure is aimed to design a separation where either the minimum amount of stationary phase is used to separate a given amount of feed or the maximum amount of feed is separated in a given SMB unit with a fixed stationary phase inventory [13]. In both cases, one has to maximize the productivity of the unit, which is defined as the mass of pure product recovered per unit time and unit mass of stationary phase:

$$PR = \frac{Q_F c_T^F}{(1 - \varepsilon^*)\rho_s V_T} \tag{41}$$

where V_T is the overall volume of the separation unit and ρ_s is the solid bulk density. With reference to SMB units, using Eq. (7) yields the following relationship:

$$PR = \frac{c_T^F (m_3 - m_2)}{\rho_s t^* \sum_{j=1}^{4} S_j} \tag{42}$$

3.2. Optimal operating conditions

In this section we are interested in determining the optimal operating conditions for a given feed composition within the region of complete separation in the operating parameter space spanned by the flow-rate ratios m_j, $j = 1,...,4$. In particular, the location of the optimal operating point in the (m_2, m_3) plane is looked for. Optimal operating conditions are defined with reference to the above performance parameters, hence they correspond to minimum desorbent requirement and maximum enrichment and productivity.

Let us refer to the relationships giving the performance parameters in terms of the m_j values, i.e. Eqs. (38–40,42). It is readily observed that all performance parameters improve by increasing the difference $(m_3 - m_2)$, i.e. by moving the operating point from the diagonal towards the vertex w of the complete separation region across straight lines of unitary slope in the (m_2, m_3) plane (see Fig. 5). It follows that the point w represents optimal operating conditions as far as only flow-rate ratios m_2 and m_3 are considered. If the relationships corresponding to the Langmuir isotherm are used, the coordinates of the optimal point are:

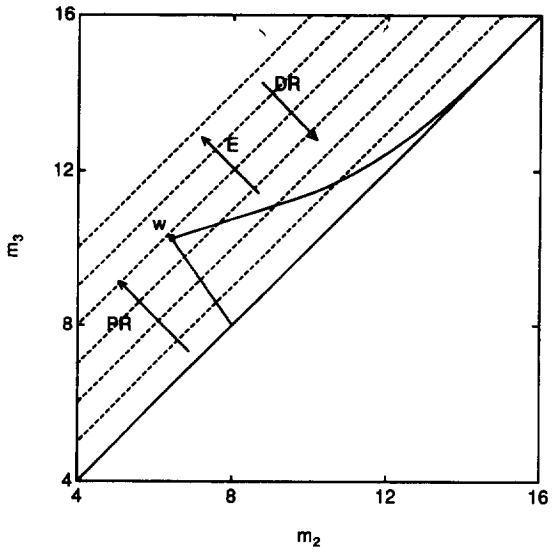

Fig. 5. Separation of a two component mixture using a nonadsorbable desorbent. Region of complete separation in the (m_2, m_3) plane, together with a series of lines with unitary slope [corresponding to constant values of the difference $(m_3 - m_2)$].

$$m_{2,opt} = \frac{\gamma_B \omega_G}{\gamma_A} \tag{43}$$

$$m_{3,opt} = \frac{\omega_G[\omega_F(\gamma_A - \gamma_B) + \gamma_B(\gamma_B - \omega_F)]}{\gamma_B(\gamma_A - \omega_F)} \tag{44}$$

Let us deepen the analysis by considering the other operating parameters appearing in the above performance parameters relationships. For optimal values of m_2 and m_3, desorbent requirement and enrichment of A and B improve if m_1 is small and m_4 is large. It follows that the optimal values of m_1 and m_4 coincide with their lower and upper bounds, respectively, which in the case of the Langmuir isotherm are given by Eq. (18) and Eq. (20), i.e.:

$$m_{1,opt} = m_{1,min} = \gamma_A \tag{45}$$

$$m_{4,\mathrm{opt}} = m_{4,\max} = \frac{1}{2}\left\{\gamma_B + m_3 + K_B c_B^F (m_3 - m_2) - \sqrt{[\gamma_B + m_3 + K_B c_B^F (m_3 - m_2)]^2 - 4\gamma_B m_3}\right\} \quad (46)$$

For linear systems, the same considerations about performance parameters lead to the following optimal flow-rate ratios: $m_{1,\mathrm{opt}} = m_{3,\mathrm{opt}} = \gamma_A$; $m_{2,\mathrm{opt}} = m_{4,\mathrm{opt}} = \gamma_B$. For systems characterized by the modified Langmuir isotherm (32) the optimal values of the flow-rate ratios are obtained by adding the linear term coefficient h to the right hand sides of Eqs. (43–46).

According to Eq. (42), the smaller the value of the switch time t^* the larger the productivity. In principle, if t^* vanishes productivity will approach infinity. In practice, this physically unrealistic result is a consequence of the fact that the equilibrium theory model that is being used assumes that the columns have infinite efficiency. As a matter of fact, this is only an approximation which is valid only when the characteristic time of mass transport and that of axial dispersion are much smaller and larger, respectively, than the residence time in the columns. These conditions are not fulfilled when t^* becomes too small and the internal flow-rates in the SMB units become too large, in order to keep the same operating point in terms of flow-rate ratios m_j according to Eq. (7). As a consequence, the optimal value of the switch time t^* can be chosen only on the base of a detailed model of the SMB unit which accounts for mass transport resistances and axial mixing [13].

It is noteworthy that for known values of t^* and of the physical parameters, such as solvent and solid densities, using Eqs. (43–46) the exact values of the performance parameters given by Eqs. (38–40,42) can be calculated explicitly in the optimal operating point as functions of the feed composition. This allows a thorough analysis of the role of the nonlinearity induced by changes of feed composition on the separation performances of the SMB unit; this issue will be dealt with in Section 4.

3.3. Robust operating conditions

Under the optimal operating conditions derived in the previous section the performance of the unit is very sensitive to various kinds of disturbances, such as perturbations in the operating conditions, inaccuracies in the chemico-physical parameters and model uncertainties; in other words these conditions are not robust [11]. By robust conditions it is meant that small disturbances do not modify the qualitative behavior of the unit. With reference to complete separation conditions, this means that as a consequence of the disturbance the actual performances change, but the unit still achieves complete separation. Robustness is of great importance in choosing operating conditions for practical applications, because sensitive operating conditions must be avoided in industrial plants.

Either perturbations in the operating conditions, i.e. flow-rates, Q_j^{SMB}, and switch time, t^*, or inaccuracies in the estimation of geometrical features of the columns, such as volume, V, and overall void fraction of the bed, ε^*, may modify the flow-rate ratios m_j defined by Eq. (7). Thus the operating point may be carried from the expected location in the complete separation region, to another position which is likely to be outside the complete separation region itself. In practice, the minimum distance of the operating point from the boundaries of the complete separation region is a measure of the maximum acceptable perturbation on the value of the flow-rate ratios m_j [11]. The further from the boundaries of the complete separation region the designed operating point, the more robust the operating conditions.

On the other hand, perturbations in the feed composition modify the shape and location of the complete separation region according to Eqs. (18–29), whereas they have no impact on the values of the flow-rate ratios m_j. The same effect may be caused by model uncertainties, such as poor estimations of either the equilibrium constants, K_i, or the saturation adsorbed phase concentrations, N_i. Another situation may rather often occur, when the adsorption isotherms characterizing the system under examination are only rather poorly approximated by one of the adsorption isotherms that we have analyzed in the previous section and for which the complete separation region can be calculated through simple algebraic relationships. In this case the complete separation region cannot be determined exactly

for the real system and the region calculated using the approximated Langmuir equilibrium model may be more or less different from the real one. In all the above mentioned cases the expected complete separation region, within which the operating point has been chosen, is different from the actual complete separation region, which may not include the selected operating point. Also in this case, if the operating point is rather far from the optimal point it is likely that small perturbations and inaccuracies do not hinder the separation. This effect is illustrated in Fig. 6, where the dashed lines are the boundaries of the complete separation region calculated using the estimated values of the equilibrium parameters. Two operating points have been chosen within the estimated complete separation region: point 1 is very close to the vertex of the region and corresponds to complete separation with good values for all the other performance parameters defined above; on the contrary point 2 is still in the estimated complete separation region but rather far from the optimal point and the corresponding separation performances are poorer than in point 1. The solid lines are the boundaries of the real complete separation region,

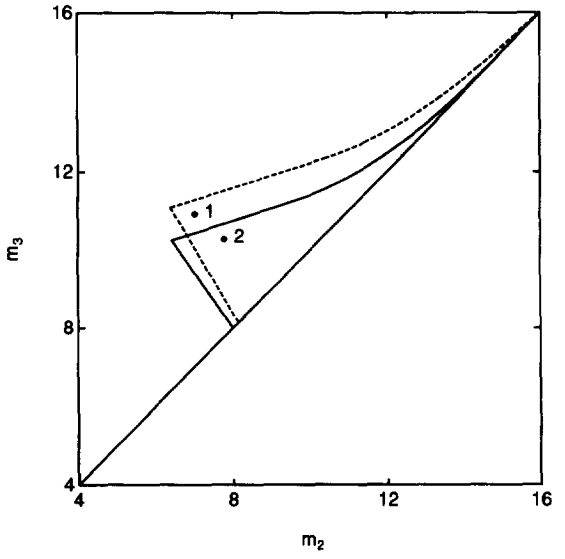

Fig. 6. Effect of errors in the estimation of the equilibrium parameters on the location of the complete separation region; $c_A^F = 1.2$ g/l, $c_B^F = 0.8$ g/l. (———) real complete separation region: $N_A = 50$ g/l, $N_B = 40$ g/l, $K_A = 0.3$ l/g, $K_B = 0.2$ l/g. (– – –) estimated complete separation region: $N_A = 51$ g/l, $N_B = 37$ g/l, $K_A = 0.33$ l/g, $K_B = 0.22$ l/g. (●): operating points.

which is not known in practical applications and in this example has been calculated using values of the equilibrium parameters which differ by no more than 10% from the estimated ones. It is readily observed that point 1 does not belong to the real complete separation region, but it is located in the pure extract region, thus failing to achieve complete separation as expected. On the contrary, point 2 belongs also to the real complete separation region, thus succeeding to achieve complete separation.

From these considerations it is straightforward that the optimal point w in the (m_2, m_3) plane is not robust at all, since the slightest disturbance can drive the operating point in one of the three separation regions where complete separation is not achieved (cf. Fig. 4). As shown above, robustness of the operation can only be improved at the expense of separation performances, by choosing a point within the complete separation region far enough from the optimal point. How far this point must be selected depends on the expected magnitude of the perturbations and on the shape of the complete separation region. In fact, by comparing Figs. 3 and 4 it is rather evident that the robustness of the separation increases with increasing values of the angle between the straight lines emanating from the optimal point, i.e. lines wa and wb in Fig. 3 and lines wf and wb in Fig. 4. On the other hand, the robustness decreases when the distance between the optimal point w and the diagonal decreases. By combining these two information about the optimal point, i.e. angle and distance, which can be directly calculated from the coordinates of the optimal point itself, an estimation of the overall robustness of the separation under examination can be obtained. In other words, this parameter provides an indication of the loss of separation performances (in terms of desorbent requirement, enrichment and productivity) that must be accepted in order to operate the unit in robust conditions with respect to complete separation. This quantitative measure of robustness will be exploited in the following section.

4. Effect of nonlinearity on the separation performances of SMB units

In the previous sections criteria for the choice of

optimal and robust operating conditions to achieve complete separation have been derived for both linear and nonlinear (of the Langmuir and modified Langmuir type) systems. Moreover it has been pointed out that the Langmuir isotherm approaches linear behavior when the concentration of the adsorbable species becomes smaller and smaller; this occurs in a SMB unit when the components to be separated become more and more diluted in the feed, i.e. when $c_T^F \to 0$.

In this section we are interested in studying the role of nonlinearity on the separation performances of SMB units under the effect of changes, either of the overall feed concentration, c_T^F, or of the relative composition of the two components to be separated. To this aim, let us define the solvent free mass fraction of component i in the feed as:

$$x_i^F = \frac{c_i^F}{c_T^F} \tag{47}$$

since for a binary separation $(x_A^F + x_B^F) = 1$ it follows that the composition of the feed mixture can be univocally identified by two independent parameters, which can be either c_A^F and c_B^F or else c_T^F and x_A^F. The former were used in Eqs. (18–29), whereas the latter will be used in the following.

4.1. Effect of feed concentration

The role of the overall feed concentration, c_T^F, is analyzed by considering how the complete separation region and the separation performances change when this parameter is varied. Since the Langmuir adsorption isotherm (16) exhibits linear behavior in the limiting case of very dilute systems, the complete separation region obtained in Section 2.2 design for systems described by the Langmuir isotherm should approach the complete separation region corresponding to a system characterized by the linear isotherm (10) with $H_i = \gamma_i$ in the limit of vanishing feed concentration values.

First, let us consider the flow-rate ratio m_1; in this case the property conjectured above is trivially verified since the nonlinear constraint (18) coincides with the linear one (11), whatever the value of the feed concentration is. This is a consequence of the fact that the desorbent is nonadsorbable.

Secondly, consider the upper bound on the flow-rate ratio m_4 given by Eq. (20), i.e. $m_{4,\max}$, which, contrary to the case of $m_{1,\min}$, is a function of c_T^F. By analyzing Eq. (20) it is readily observed that $m_{4,\max} = \gamma_B$ when $c_T^F = 0$, whereas for any other value of the feed concentration $m_{4,\max} < \gamma_B$. Thus, under infinite dilution conditions the nonlinear inequality (20) coincides with the linear constraint (14), as expected. These results prove that large feed concentrations imply small upper bounds on the flow-rate ratio m_4, and vice versa. This means that smaller values of the flow-rate ratio in section 4 are required in order to avoid that more concentrated breakthrough fronts of the two species reach the outlet of section 4 itself within a time period between two successive switches of the inlet and outlet ports. This effect is a consequence of the well known property of favourable isotherms, such as the Langmuir isotherm, for which the propagation velocity of concentration states increases with increasing values of concentration.

Finally, let us analyze the effect of the overall feed concentration on the shape and location of the complete separation region in the (m_2, m_3) plane. To this aim one has to calculate the complete separation region for the same separation, i.e. same values of the solvent free mass fraction x_A^F and of the adsorption equilibrium parameters K_i and N_i, but for different values of the overall feed concentration, c_T^F. This can simply be done using the equations derived in Section 2 in the nonlinear case, i.e. Eqs. (21–29); the results are illustrated in Fig. 7. Five complete separation regions are shown, going from region L, corresponding to the limiting situation of a feed mixture constituted of A and B infinitely diluted in the solvent, to regions I to IV, corresponding to larger and larger values of the feed concentration. As conjectured, region L coincides with the linear complete separation region defined by Eq. (12) and Eq. (13), with $H_i = \gamma_i$, and the other regions approach it when c_T^F decreases, i.e. in going from region IV to region I. This property can also be demonstrated by calculating the expressions (or their limits when necessary) appearing in Eqs. (21–29) when $c_T^F = 0$ (or when $c_T^F \to 0$); in this case the roots of Eq. (30) are $\omega_F = \gamma_B$ and $\omega_G = \gamma_A$, points r, f and a collapse in a single point and the coordinates of the optimal point w are γ_B and γ_A as in the linear case.

Some insights about the choice of the operating conditions of SMB units can be obtained by deepen-

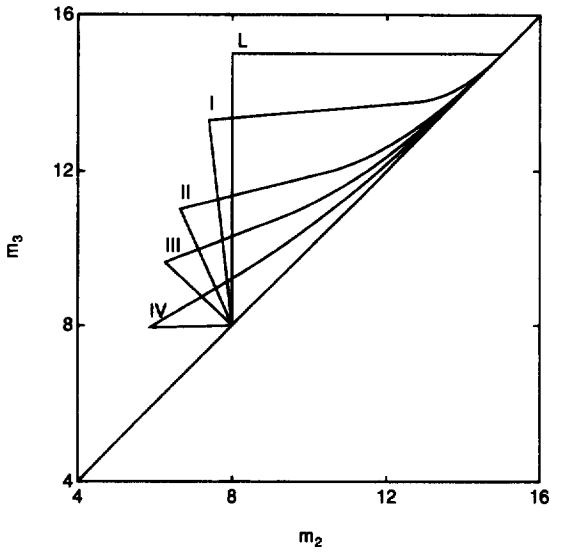

Fig. 7. Effect of the overall concentration of the feed mixture, c_T^F, on the region of complete separation in the (m_2, m_3) plane. $N_A=50$ g/l, $N_B=40$ g/l, $K_A=0.3$ l/g, $K_B=0.2$ l/g, $c_A^F=x_A^F c_T^F$, $c_B^F=c_T^F-c_A^F$, $x_A^F=0.6$. (L) $c_T^F\to 0$ g/l, i.e. linear system; (I) $c_T^F=0.5$ g/l; (II) $c_T^F=1.5$ g/l; (III) $c_T^F=2.5$ g/l; (IV) $c_T^F=5$ g/l.

ing the analysis of Fig. 7. First, the intersection of the complete separation region with the diagonal in the (m_2, m_3) plane remains the same whatever the value of the feed concentration is. In fact for both very diluted and very concentrated feed mixtures when the operating point gets closer and closer to the diagonal the feed flow-rate, which is proportional to the difference (m_3-m_2), approaches zero. Under these conditions, even though the concentration of the feed mixture is large, the concentration of the components to be separated within the unit is very small, and the operating conditions to achieve complete separation become the same as those of region L, thus achieving the same conditions as in the case of infinite dilution linear systems. The upper bound on m_4 given by Eq. (20) exhibits the same effect, since it approaches γ_B when (m_3-m_2) vanishes.

Secondly, while c_T^F increases, the position of the optimal point w changes moving towards the lower left corner of the (m_2, m_3) plane. At the same time the complete separation region becomes smaller and sharper with a long tail oriented towards the upper right corner of the (m_2, m_3) plane. In other words, the complete separation region gains an increasing nonlinear character. It follows that, in order to maintain optimal performances when the overall feed concentration increases, decreasing values of the fluid to solid flow-rate ratio both in sections 2 and 3 must be selected. A physical interpretation of this feature of the separation process can be provided following an argument similar to the one given above to explain the corresponding decrease of the value of $m_{4,max}$.

Other information can be obtained by considering how the performance parameters defined in the previous section change while the overall feed concentration increases. It is worth comparing the values of the performance parameters corresponding to the optimal operating point for a given value of the overall feed concentration. These represent the maximum achievable separation performances for the given value of feed concentration, hence a good basis for comparison among the results obtained for the different values of feed concentration be considered.

In Fig. 8 the enrichments of A in the extract and of B in the raffinate, defined by Eqs. (39) and (40), respectively, are plotted as a function of the overall

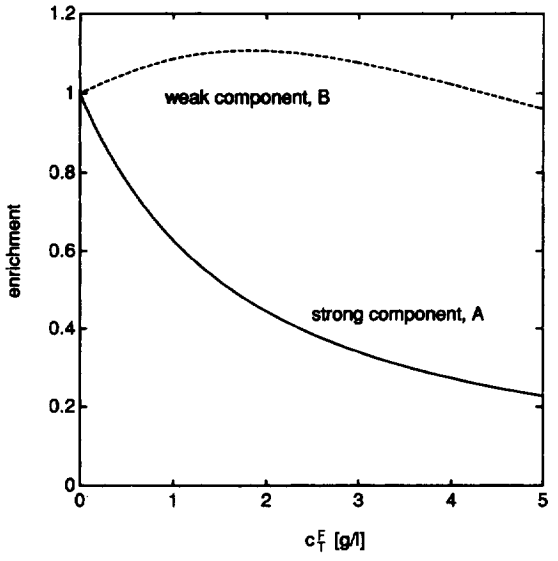

Fig. 8. Effect of the overall concentration of the feed mixture, c_T^F, on the enrichment of the outlet streams: (———) enrichment of component A in the extract; (– – –) enrichment of component B in the raffinate. $N_A=50$ g/l, $N_B=40$ g/l, $K_A=0.3$ l/g, $K_B=0.2$ l/g, $c_A^F=x_A^F c_T^F$, $c_B^F=c_T^F-c_A^F$, $x_A^F=0.6$.

feed concentration, c_T^F. The relationship used to calculate the curve corresponding to the enrichment of B is the following one:

$$E_B = \frac{m_{3,opt} - m_{2,opt}}{m_{3,opt} - m_{4,opt}} \quad (48)$$

where the values of $m_{j,opt}$, $j=1,...,4$, are calculated through Eqs. (43–46) as functions of c_T^F. The enrichment of A in the extract is calculated accordingly, turning out to be less than 1 for every positive value of c_T^F. This is a consequence of the desorbent being nonadsorbable, thus imposing large flow-rates in section 1 in order to elute component A completely. Most of the solvent used in section 1 is then withdrawn in the extract, thus diluting component A whose concentration in the extract can never even reach that in the feed. On the contrary, the enrichment of component B first increases until it reaches a maximum where the outlet concentration is larger than its feed concentration; then it decreases approaching zero more slowly than the enrichment of A. This is a typical nonlinear effect which is justified by the rather complex relationship, i.e. Eq. (48), which gives E_B as a function of c_T^F.

Finally. let us consider the behavior at zero overall feed concentration, i.e. under linear conditions. Both enrichment values are equal to one, since they are calculated in the optimal point where $m_{1,opt} = m_{3,opt} = \gamma_A$ and $m_{2,opt} = m_{4,opt} = \gamma_B$. However, on the basis of the definition of the enrichment parameters it is readily observed that if the operating conditions are chosen within the complete separation region, i.e. fulfilling the constraints (11) to (14), but they do not correspond to the optimal conditions, then the enrichments of both species are smaller than one.

The behavior of desorbent requirement and productivity as functions of the overall feed concentration are illustrated in Fig. 9, together with the corresponding behavior of the parameter giving a quantitative account of the robustness of the complete separation region. All these parameters are calculated analytically using their definitions and the optimal values of the flow-rate ratios m_j given by Eqs. (43–46); constant values of all the other parameters appearing in Eqs. (38) and (42) have been used. It can be observed that both productivity and desorbent consumption improve monotonically for increasing values of feed concentration, approaching finite

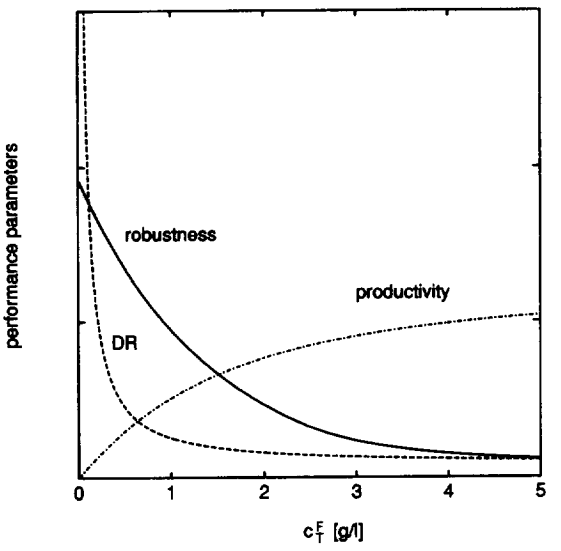

Fig. 9. Effect of the overall concentration of the feed mixture, c_T^F, on the separation performances: (———) robustness; (– – –) desorbent requirement; (– · –) productivity. $N_A = 50$ g/l, $N_B = 40$ g/l, $K_A = 0.3$ l/g, $K_B = 0.2$ l/g, $c_A^F = x_A^F c_T^F$, $c_B^F = c_T^F - c_A^F$, $x_A^F = 0.6$.

asymptotic values. This is not a trivial result, since two counteracting effects are active: the first one is the increase in feed concentration which has a positive impact on both parameters; the second one is the change in the position of the optimal point w in the (m_2, m_3) plane which gets further and further to the diagonal, thus causing a decrease of the difference $(m_3 - m_2)$ and consequently a worsening of both performance parameters. Thus concluding, the first effect prevails and large feed concentrations would be recommended if only these two performance criteria were considederd. However, it should be noticed that after a rather small value of the feed concentration is reached both desorbent requirement and productivity get rather close to their asymptotic limits, hence further increases of feed concentration have very little positive effects on these two key parameters. On the contrary, robustness monotonically decreases with increasing feed concentration; its asymptotic limit is zero. This behavior is a consequence of the marked sharpening of the complete separation region in going from small to large feed concentrations, as observed above with reference to Fig. 7, together with the approach to the diagonal of the optimal point w. Both effects have a negative

impact on the robustness of the separation, as already observed in Section 3.3.

Thus summarizing, the optimal value of the overall feed concentration, c_T^F, must be chosen on the basis of a compromise among the different tendencies of the above discussed performance parameters; in particular between productivity and desorbent requirement, which suggest large values of c_T^F, and robustness, which is optimized at small values of the feed concentration. The quantitative account of these effects provided by the explicit expressions developed in this work can be very helpful in determining these optimal conditions.

Robustness deserves a final comment. At large feed concentration the operation of the unit is not very robust, as clearly illustrated in Fig. 7 and Fig. 9. This means not only that the performance of the unit is very sensitive to perturbations but also that it would be very difficult to choose operating conditions to achieve complete separation if no information about the location of the complete separation region in the operating parameter space were available. In practice, one would be forced to operate at rather small values of feed concentration, thus achieving low productivity with large desorbent consumption. On the contrary, the knowledge of the complete separation region obtained by applying the approach presented in this work gives the possibility of finding proper operating conditions to achieve complete separation also at large feed concentration. As a consequence, better values of desorbent requirement and productivity than if these information were not available can be reached.

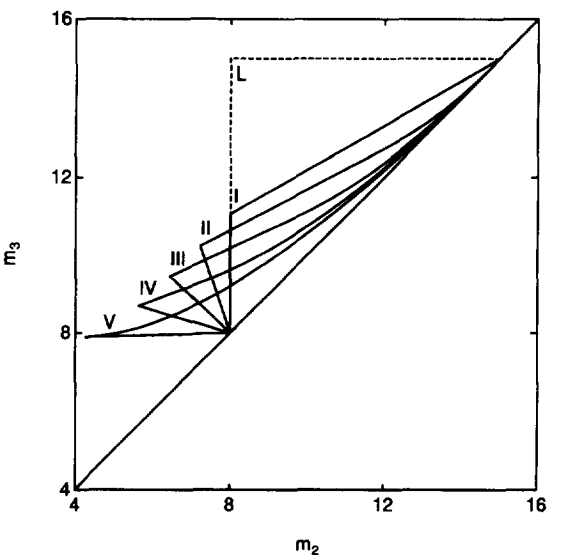

Fig. 10. Effect of the relative composition of the feed mixture on the region of complete separation in the (m_2, m_3) plane. $N_A = 50$ g/l, $N_B = 40$ g/l, $K_A = 0.3$ l/g, $K_B = 0.2$ l/g, $c_A^F = x_A^F c_T^F$, $c_B^F = c_T^F - c_A^F$, $c_T^F = 3$ g/l. Region L (dashed boundaries): linear region of complete separation. (I) $x_A^F \to 0$; (II) $x_A^F = 0.25$; (III) $x_A^F = 0.50$; (IV) $x_A^F = 0.75$; (V) $x_A^F \to 1$.

4.2. Effect of feed composition

In this section the effect of changes of the relative feed composition of the two components to be separated at constant overall feed concentration, c_T^F, is analyzed. This is an effect of the nonlinear character of the separation, since for systems described by linear adsorption isotherms the feed composition plays no role in determining the region of complete separation, as demonstrated in Section 2.1. The possibility of changing the relative feed composition is limited to cases where the adsorptive separation is preceeded by a reaction stage or a separative pretreatment whose outlet composition can be rather freely tuned.

In Fig. 10, five complete separation regions calculated for the same separation but different values of the solvent free mass fraction of the strong component A in the feed, x_A^F, are drawn in the (m_2, m_3) plane. In going from region I to region V x_A^F increases from 0 to 1, with regions II to IV corresponding to x_A^F equal to 0.25, 0.5 and 0.75, respectively. The linear region of complete separation has also been drawn with dashed boundaries for comparison. It can readily be noticed that in this case also the intersection between the complete separation region and the diagonal remains the same, since it corresponds to infinite dilution conditions within the separation unit. The optimal point, i.e. the vertex of the triangle-shaped region w, moves downwards to the left, but its distance from the diagonal does not change much. In the particular example illustrated in Fig. 10 the relative variation of this distance between regions I and V is only about 10%. As a consequence, productivity and desorbent consumption remain

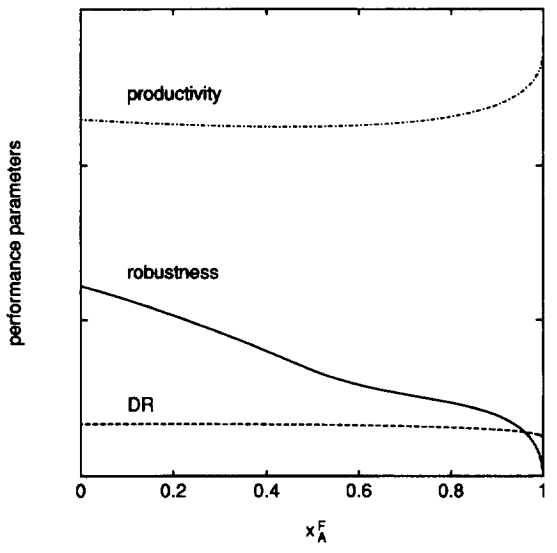

Fig. 11. Effect of the relative composition of the feed mixture on the separation performances: (———) robustness; (– – –) desorbent requirement; (– · –) productivity. $N_A=50$ g/l, $N_B=40$ g/l, $K_A=0.3$ l/g, $K_B=0.2$ l/g, $c_A^F=x_A^F c_T^F$, $c_B^F=c_T^F-c_A^F$, $c_T^F=3$ g/l.

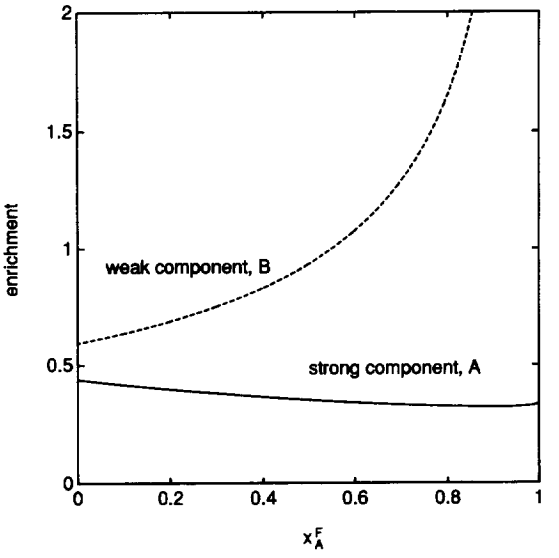

Fig. 12. Effect of the relative composition of the feed mixture on the enrichment of the outlet streams: (———) enrichment of component A in the extract; (– – –) enrichment of component B in the raffinate. $N_A=50$ g/l, $N_B=40$ g/l, $K_A=0.3$ l/g, $K_B=0.2$ l/g, $c_A^F=x_A^F c_T^F$, $c_B^F=c_T^F-c_A^F$, $c_T^F=3$ g/l.

roughly constant for the whole range of relative feed composition, as illustrated in Fig. 11.

However, the movement of the optimal point in the (m_2, m_3) plane yields a marked distortion of the complete separation region, which becomes smaller and sharper as the solvent free weight fraction of component A increases. Accordingly, the robustness of the separation decreases, as illustrated in Fig. 11. This asymmetric behavior is clearly due to the nonadsorbable nature of the desorbent; calculations not reported here indicate that in the case of a desorbent with a larger adsorptivity than both components to be separated the opposite behavior occurs, i.e. the complete separation region gets sharper as the solvent free mass fraction of component B increases.

As far as enrichment effects are concerned, by inspection of Fig. 12 it can be shown that the enrichment of component A in the extract is mildly affected by changes of relative composition of the feed mixture. On the contrary, the effect of these changes on the enrichment of B in the raffinate is important: values of this parameter much larger than 1 can be obtained when the relative amount of A in the feed is larger than that of B.

5. Comparison with experimental results

In this section, the above developed criteria for the design of the operating conditions to achieve complete separation are assessed by comparison with SMB experimental data reported in the literature. This allows the full appreciation of the usefulness of the theoretical results demonstrated in this work. In particular, the results presented by Küsters et al. [9] and by Charton and Nicoud [10] about the separation of two different racemic mixtures are discussed.

5.1. Separation of the Sandoz chiral epoxide

First, let us consider the experimental data referring to the separation on the chiral stationary phase Chiralcel-OD of the racemic epoxide (±)-1a,2,7,7a-tetrahydro-3-methoxynaphth-(2,3*b*)-oxirene [9]. This is the so-called Sandoz epoxide, which is an intermediate in the asymmetric synthesis of some optically active drugs; its separation has been considered as a case study in a number of publications [8,21].

The experimental adsorption equilibrium data

reported by the authors [9] have been fitted using the constant selectivity Langmuir adsorption isotherm (16); the following values of the equilibrium parameters have been estimated (the subscripts A and B refer to the (−) and the (+) enantiomer, respectively): $N_A = 165$ g/l; $N_B = 220$ g/l; $K_A = 0.0321$ l/g; $K_B = 0.0175$ l/g. The calculated competitive isotherms are compared with the experimental data in Fig. 13, showing a good agreement for single enantiomer concentrations smaller than 10 g/l, which is the range adopted in the reported SMB experiments. The poor agreement observed for larger values of the feed concentration does not affect the following analysis.

The SMB experiments have been run in a 12 port pilot unit (3-3-3-3 configuration) using *n*-hexane–isopropanol (9/1) as mobile phase; the following geometric and operating parameters have been indicated [9]: $V = 20.1 \cdot 10^{-3}$ l; $\varepsilon^* = 0.67$; $t^* = 780$ s. Two different overall racemate feed concentrations have been adopted, namely a low and a high level corresponding to 5 and 20 g/l, respectively. By applying the theory developed in Section 2 and using Eqs. (21–29), two different complete separation regions in the (m_2, m_3) plane are obtained: region S and region G corresponding to $c_T^F = 5$ g/l and $c_T^F = 20$ g/l, respectively. These regions are drawn in Fig. 14, along with the linear complete separation region (region L) obtained by letting $c_T^F \to 0$. It is noteworthy how different are the three complete separation regions and how far the three corresponding optimal points are in the (m_2, m_3). The operating points representing the reported experimental runs are also indicated; their coordinates have been calculated by substituting the experimental values of the flow-rates reported by the authors into Eq. (7). The experimental values of the flow-rate ratios m_j and of the obtained purities of the product streams are reported in Table 1, together with the values of feed concentrations. Note that runs 1 and 2 share the same operating point, but with different values of the feed concentration. In the same table, the critical values of the flow-rate ratios m_1 and m_4 calculated using Eq. (18) and Eq. (20), respectively, are reported in brackets next to the corresponding experimental values. This allows the observation that in all the experimental runs the operating values of m_1 and m_4 fulfil the relevant constraints. Therefore, we can perform the analysis of these experimental data by

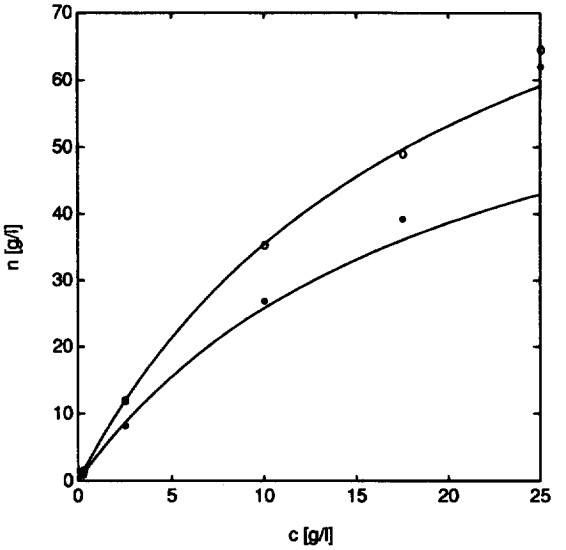

Fig. 13. Experimental [9] and calculated adsorption isotherms for the Sandoz epoxide enantiomers on Chiralcel-OD. ○: (−)enantiomer; ●: (+)enantiomer.

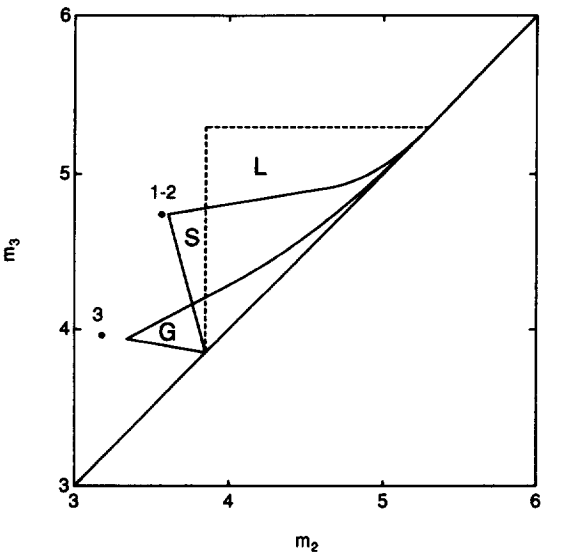

Fig. 14. Separation of the chiral epoxide in a SMB pilot unit [9]. Comparison of the predicted regions of complete separation in the (m_2, m_3) plane with the experimental data (●). Region L (dashed boundaries): linear region of complete separation. Region S: $c_T^F = 5$ g/l. Region G: $c_T^F = 20$ g/l. The location of point 1 must be compared with region S, whereas those of points 2 and 3 with region G.

Table 1
Separation of the chiral epoxide in a SMB pilot unit: flow-rate ratios and separation performances of the experimental runs [9]

Run	Feed racemate concentration (g/l)	Flow-rate ratios				Experimental purity values	
		m_1 ($m_{1,\min}$)	m_2	m_3	m_4 ($m_{4,\max}$)	P_E (%)	P_R (%)
1	5	5.52 (5.3)	3.56	4.74	2.77 (3.67)	98.2	96.5
2	20	5.52 (5.3)	3.56	4.74	2.77 (3.35)	93.8	43.0
3	20	5.52 (5.3)	3.17	3.96	2.40 (3.23)	94.4	95.0

The critical values of the flow-rate ratios in sections 1 and 4 calculated using Eq. (18) and Eq. (20) are reported in brackets next to the corresponding operating values.

simply considering the relative position of the operating points in Fig. 14 with respect to the two predicted regions of complete separation. Since the feed concentration values are different in the three experimental runs, it follows that the position of point 1 must be compared with the region S, calculated for a 5 g/l feed concentration, whereas the position of points 2 and 3 with region G, determined for a 20 g/l feed concentration.

First, let us consider run 1 and note that its operating point is very close to the optimal operating point of region S. This is in good agreement with the achieved experimental performance, corresponding to purities between 96% and 98% in both product streams; purity values are pretty good but complete separation has not been fully achieved since the optimal point is not robust and very sensitive to disturbances. A similar argument may be followed to comment upon the results obtained during the experimental run 3, whose operating point is close to the optimal operating point of region G. Moreover, point 3 is further from the optimal point than point 1 and it is located well within the region where neither outlet stream is pure; in fact even though the outlet purities are pretty large, i.e. around 95%, undoubtedly complete separation has not been achieved. Now, let us consider run 2; as discussed in Section 4, increasing the feed concentration from 5 to 20 g/l produces a rather large shift of the complete separation region (from region S to region G). It follows that the operating point 2, which coincides with the operating point 1, is no more close to the optimal location of the complete separation region which corresponds to its feed concentration value, i.e. region G. Recalling Fig. 4, it is readily observed that point 2 is in the region of the (m_2, m_3) plane where the raffinate purity drops. This is in very good agreement with the experimental results, which indicate a large decrease of raffinate purity from 96.5% in run 1 to 43% in run 2.

5.2. Resolution of the EMD 53986 enantiomers

The second example deals with the resolution of the EMD 53986 enantiomers, which is a synthesis chiral intermediate. The separation has been performed by Charton and Nicoud [10] in a 12 port SMB pilot unit using Celluspher as stationary phase, a chiral stationary phase prepared from cellulose tri(*p*-methylbenzoate), and pure methanol as mobile phase. The following geometric and operating parameters have been reported by the authors: $V = 45.13 \cdot 10^{-3}$ l; $\varepsilon^* = 0.358$; $t^* = 792$ s.

The experimental competitive adsorption equilibrium data have been described by the authors using a variable selectivity modified Langmuir isotherm (32), according to the following relationships:

$$c_A = 3.96 c_A + \frac{15.96 c_A}{1 + 0.317 c_A + 0.140 c_B} \quad (49)$$

$$c_B = 3.96 c_B + \frac{7.07 c_B}{1 + 0.317 c_A + 0.140 c_B} \quad (50)$$

Only one SMB experimental run has been reported [10]; this has been performed at an overall feed concentration of 7.5 g/l. The corresponding nonlinear region of complete separation (solid boundaries) has been calculated, following the procedure demonstrated in Section 2.3, and drawn in Fig. 15, together with the linear complete separation region (dashed boundaries) and with the operating point X. The values of the flow-rate ratios m_j

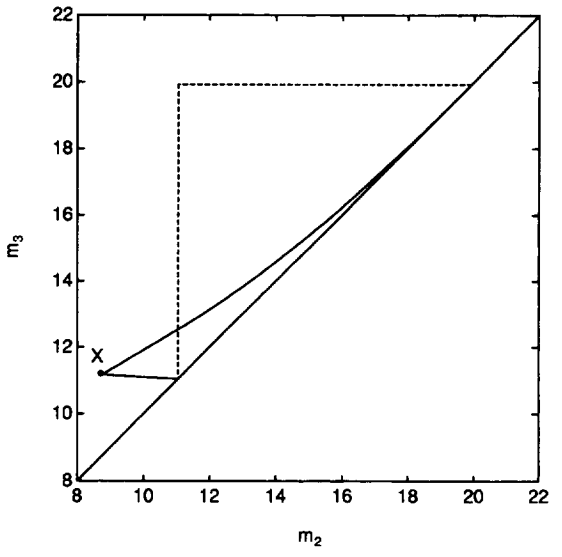

Fig. 15. Separation of the EMD 53986 enantiomers in a SMB pilot unit [10]. Comparison of the predicted region of complete separation in the (m_2, m_3) plane with the experimental operating point (●). (– – –): boundaries of the corresponding linear complete separation region.

adopted in run X and calculated substituting the values of the experimental flow-rates in Eq. (7) are reported in Table 2, together with the experimental values of the purities obtained in the outlet streams. It is worth recalling that according to the authors the experimental operating point has been chosen with the objective of achieving at least 99% purity in both product streams [10]. In the second row of Table 2 the flow-rate ratios corresponding to the optimal operating point calculated using Eq. (35) and Eqs. (43–46) are indicated; by definition, complete separation performances are assumed to be achieved under these theoretical operating conditions.

It is apparent from both Fig. 15 and Table 2 that the operating point X coincides with the optimal operating point predicted by the theory. According to the analysis developed in Section 3.3 about the issue of robust operating conditions it is not surprising that the experimental purities are not better than 97%. As a matter of fact, operating the separation in the optimal point of such a nonlinear region of complete separation (note the big shift in the position of the nonlinear reagion with respect to the linear one) makes the operation too sensitive to disturbances. In this case we guess that the main cause of disturbances may be related to uncertainties in the description of the competitive adsorption equilibrium. In fact only five equilibrium measurements have been performed on the racemic mixture (corresponding to ten equilibrium data) and have been used to estimate the five parameters appearing in Eq. (49) and Eq. (50) [10].

6. Concluding remarks

The continuous chromatographic separation of mixtures in an SMB unit has been studied. After more than thirty years of industrial practice in the field of hydrocarbon and sugar separations, this technology is now being paid great attention in view of its application to difficult fine chemistry separations. In general, the design of the operating conditions of SMB units to achieve the prescribed separation performances is rather difficult, because of their complex behavior and of the strong nonlinear competitive equilibrium effects which are often exhibited [10]. As a consequence, there is a tendency either to operate under rather diluted conditions in order to minimize the nonlinear effects or else to search the operating parameter space for optimal nonlinear operating conditions in a rather empirical way [9].

Table 2
Separation of the EMD 53986 enantiomers in a SMB pilot unit: flow-rate ratios and separation performances of the experimental run X [10]

Run	Feed racemate concentration (g/l)	Flow-rate ratios				Purity values	
		m_1	m_2	m_3	m_4	P_E (%)	P_R (%)
X	7.5	19.90	8.78	11.24	8.74	~97	~97
optimum	7.5	19.92	8.76	11.16	8.66	100	100

The operating parameters in the second row of the table correspond to optimal operating conditions.

In this paper, we have presented a general theory which allows to solve this problem. In particular, explicit criteria for the choice of the operating conditions of SMB units to achieve the prescribed separation of a binary mixture characterized by both constant selectivity Langmuir isotherms (16) and variable selectivity modified Langmuir isotherms (32) have been derived. It has been demonstrated that the space of the operating parameters, i.e. the fluid to solid flow-rate ratios m_j, is divided in four regions with different separation regimes. In particular, the boundaries of the complete separation region are calculated through explicit relationship which involve the adsorption equilibrium parameters of the components to be separated. Several performance parameters have been introduced, namely desorbent requirement, enrichment of the components to be separated in the product streams and productivity. By analyzing the behavior of these parameters while changing the operating point the optimal conditions in the complete separation region of the operating parameter space have been determined.

The shape and location of the complete separation region in the operating parameter space as well as the values of the performance parameters obtained in the corresponding optimal operating point are determined through explicit relationships which depend on the feed composition. Since the overall feed concentration is the operating parameter through which we can control the degree of nonlinearity of the separation, a thorough analysis of the role of nonlinearity on the behavior of SMB units has been performed by simply changing the composition of the feed mixture. By doing so it can be easily discovered how to change the operating conditions, i.e. flow-rates and switch time, in order to cope with increasing values of the feed concentration and to maintain the SMB unit in the complete separation regime. This is particularly useful since both desorbent requirement and productivity improve while feed concentration increases.

A strong limitation to the increase of feed concentration is due to the corresponding decrease in the robustness of the separation. The requirement of selecting robust operating conditions for the separation has been carefully discussed, by analyzing all the possible sources of disturbances as well as the impact of increasing values of feed concentration on the overall robustness of the corresponding complete separation region. It has been shown that robustness indeed decreases while feed concentration increases. However, it must be pointed out that the availability of simple explicit expressions for the location of the complete separation region in the operating parameter space even at large values of feed concentration allows the operation of an SMB unit safely at larger feed concentration and better performances than before.

The usefulness and reliabililty of the theoretical results presented in this work have been assessed by comparison with experimental data reported in the literature and referring to the separation of the Sandoz chiral epoxide [9] and of a synthesis chiral intermediate [10]. In both cases the proposed approach has proved to be capable to predict the large shift in operating conditions necessary to cope with an increase of feed concentration and to explain, through robustness considerations, some experimental performances which were less satisfactory than expected.

We believe that the extensive adoption of criteria such as the ones presented in this work may allow the achievement of high separation performances, thus giving a strong impulse to the development of new applications of the SMB technology in the important area of fine chemicals separations.

7. Notation

c	fluid phase mass concentration
DR	desorbent requirement, defined by Eq. (37)
E	enrichment, defined by Eq. (39) and (40)
f^{eq}	adsorption equilibrium relationship
h	linear term coefficient in the modified Langmuir isotherm (32)
H	Henry constant
K	adsorption equilibrium constant
m_j	mass flow-rate ratio in section j, defined by Eq. (6) and (7)
m_j'	modified mass flow-rate ratio in section j, defined by Eq. (35)
n	adsorbed phase mass concentration
N	adsorbed phase saturation mass concentration

NC	total number of adsorbable components
P_E	desorbent free extract purity
P_R	desorbent free raffinate purity
PR	productivity, defined by Eq. (41)
q	adsorbed phase mass concentration given by the Langmuir isotherm (16)
Q	volumetric flow-rate
S_{il}	selectivity of component i with respect to component l
S_j	number of subsections in the jth section of a SMB unit
t	time
t^*	switch time in a SMB unit
V	volume of the column
x_i^F	solvent free weight fraction of component i in the feed
Y	product of column section and axial coordinate

Greek letters

γ	adsorptivity, $\gamma = NK$
ε	void fraction of the bed
ε_p	intraparticle void fraction
ε^*	overall void fraction, $\varepsilon^* = \varepsilon + \varepsilon_p(1-\varepsilon)$
ξ	dimensionless axial coordinate, $\xi = Y/V$
ρ_s	bulk solid mass density
τ	dimensionless time, $\tau = tQ_s/V$
ω	equilibrium theory parameter defined by Eq. (30)

Subscripts and superscripts

A	strong component of the feed
B	weak component of the feed
D	desorbent
E	extract
F	Feed
i,l	component indeces
j	section index
R	raffinate
s	solid phase
T	overall quantity

References

[1] D.M. Ruthven and C.B. Ching, Chem. Eng. Sci., 44 (1989) 1011.

[2] J.A. Johnson and R.G. Kabza, in G. Ganetsos and P.E. Barker (Editors), Preparative and Production Scale Chromatography, Marcel Dekker, New York, 1993.

[3] J.N. Kinkel, M. Schulte, R.M. Nicoud, F. Charton, Proceedings of the Chiral Europe '95 Symposium, Spring Innovations, Stockport, 1995, p. 121.

[4] M.J. Gattuso, B. McCulloch and J.W. Priegnitz, Chem. Tech. Eur., 3 (1996) 27.

[5] M. Mazzotti, R. Baciocchi, G. Storti and M. Morbidelli, Ind. Eng. Chem. Res., 35 (1996) 2313.

[6] G. Storti, M. Mazzotti, L.T. Furlan, M. Morbidelli and S. Carrà, Sep. Sci. Technol., 27 (1992) 1889.

[7] M. Negawa and F. Shoji, J. Chromatogr., 590 (1992) 113.

[8] R.-M. Nicoud, G. Fuchs, P. Adam, M. Bailly, E. Küsters, F.D. Antia, R. Reuille and E. Schmid, Chirality, 5 (1993) 267.

[9] E. Küsters, G. Gerber and F.D. Antia, Chromatographia, 40 (1995) 387.

[10] F. Charton and R.-M. Nicoud, J. Chromatogr. A, 702 (1995) 97.

[11] G. Storti, M. Mazzotti, M. Morbidelli and S. Carrà, AIChE J., 39 (1993) 471.

[12] M. Mazzotti, G. Storti and M. Morbidelli, AIChE J., 40 (1994) 1825.

[13] G. Storti, R. Baciocchi, M. Mazzotti and M. Morbidelli, Ind. Eng. Chem. Res., 34 (1995) 288.

[14] M. Mazzotti, G. Storti and M. Morbidelli, AIChE J., 42 (1996) 2784.

[15] D.M. Ruthven, Principles of Adsorption and Adsorption Processes, Wiley, New York, 1984.

[16] K. Hashimoto, S. Adachi, Y. Shirai and M. Morishita, in G. Ganetsos and P.E. Barker (Editors), Preparative and Production Scale Chromatography, Marcel Dekker, New York, 1993.

[17] G. Storti, M. Masi, S. Carrà and M. Morbidelli, Chem. Eng. Sci., 44 (1989) 1329.

[18] H.-K. Rhee, R. Aris and N. Amundson, Phil. Trans. Roy. Soc. London A, 269 (1971) 187.

[19] F.D. Antia and Cs. Horváth, J. Chromatogr., 556 (1991) 119.

[20] M. Mazzotti, G. Storti and M. Morbidelli, AIChE J., 43 (1997) 64.

[21] E. Küsters, Proceedings of the Chiral Europe '95 Symposium, Spring Innovations, Stockport, 1995, p. 121.